Stimulated dielectric wake-field accelerator

T-B. Zhang,[1] J. L. Hirshfield,[1,2] T. C. Marshall,[3] and B. Hafizi[1]
[1]*Omega-P, Inc., New Haven, Connecticut 06520*
[2]*Department of Physics, Yale University, New Haven, Connecticut 06511*
[3]*Department of Applied Physics, Columbia University, New York, New York 10027*

(Received 30 May 1997)

A wake-field accelerator is described based on the use of a waveguide structure in which many modes can participate in wake-field formation, and in which the wake-field period equals the period of a train of drive bunches. A dielectric-lined waveguide is analyzed that is shown to support multimode propagation with all modes having nearly equal phase velocities, equal to the initial velocity of injected charge bunches that drive the wake fields. For this waveguide, the ratio of wake field to drag field for a bare drive bunch is 4.7, as compared to 2.0 for a single-mode waveguide. The composite TM_{0n} wake field of such a structure is shown to include highly peaked axial electric fields localized on each driving bunch in a periodic sequence of bunches. This allows stimulated emission of wake-field energy to occur at a rate that is larger than the coherent spontaneous emission from a single driving bunch of equal charge and energy. This mechanism can make possible the design of a stimulated dielectric wake-field accelerator that has the potential of providing an acceleration gradient for electrons or positrons in the range of 50–100 MV/m, taking a driving bunch charge of a few nC. We present calculations for such wake fields from a bunched sheet beam in a two-dimensional dielectric waveguide. Numerical examples are given, including the acceleration of a 30 MeV test bunch to 155 MeV in a structure 200 cm in length, using ten identical 2 nC/mm drive bunches. [S1063-651X(97)03610-6]

PACS number(s): 41.60.Cr, 41.75.Ht, 29.17.+w

I. INTRODUCTION

In the conventional dielectric wake-field accelerator, a dielectric-lined waveguide supports wake fields with longitudinal electric fields induced by the passage of an electron bunch of high charge number (the ''driving bunch''). Phase velocities for the modes of dielectric-lined waveguide can be less than the speed of light [1], so that Cherenkov radiation occurs [2], manifesting itself as a wake field that fills the waveguide behind the driving bunch. If a ''test'' bunch of low charge number is injected at a suitable interval after the driving bunch, it can move in synchronism with the wake fields and experience net acceleration [3–5]. This approach for development of novel accelerators is appealing because no external source of rf power is required for acceleration, and because high-gradient longitudinal fields are predicted for achievable high intensity driving bunches. For example, Rosing and Gai [4] consider a 100 nC, 1.0 mm long driving bunch passing through a dielectric-lined waveguide with an inner radius of 2.0 mm and an outer radius 5.0 mm; they took the relative dielectric constant of the outer liner to be $\kappa=\varepsilon/\varepsilon_0=3.0$. For this they predict a peak wake-field accelerating gradient of $E_{z,\mathrm{peak}}=240$ MV/m, a value about 14 times that at the Stanford Linear Collider. Experimental confirmation of wake-field generation in a dielectric-lined waveguide has been obtained [5] using 21 MeV driving bunches of 2.0–2.6 nC and 15 MeV test bunches of much lower charge. Acceleration gradients of 0.3–0.5 MV/m were observed in the experiments, in agreement with supporting theory. Acceleration gradients in all dielectric-lined waveguides must be below the breakdown field of the dielectric [6]. This will limit achievable acceleration gradients in any dielectric-lined waveguide to a level that may not be as high as the 240 MV/m value predicted in Ref. [4].

The particular dielectric waveguide analyzed in this paper for the Stimulated Dielectric Wake-field Accelerator (S-WAC) enjoys two uncommon virtues. The first arises because many waveguide modes can participate in wake-field formation, and these are designed to have phase velocities nearly equal to one another, and to the bunch velocity. This leads to a coherent superposition of many copropagating waveguide modes, so the net wake-field amplitude can be significantly larger than amplitudes of individual modes. The second virtue arises because the near-periodic character of the wake fields allows constructive interference of field amplitudes from successive bunches. Furthermore, the analysis given here is formulated to add to the *spontaneous* Cherenkov wake-field emission of one bunch, the *stimulated* Cherenkov emission from a train of succeeding bunches. The bunches are assumed to be identical, and each bunch is injected to move initially with near synchronism in the net wake field of prior bunches. It will be shown that stimulated emission from each trailing bunch can exceed spontaneous Cherenkov emission from a bunch moving alone. Consequently, the drag field that decelerates a ''dressed'' bunch can be much larger than the drag field acting on a ''bare'' bunch. (Terms in quotes refer to the presence or absence of decelerating wake fields from prior bunches.) Thus a dressed bunch leaves behind a stronger wake than a bare bunch, and so forth for succeeding dressed bunches. Of course, the successive wake maxima are found to be not exactly periodic, and decelerating particles can slip behind the wake-field maxima; so the cumulative superposition of wakes can be less than a sum of peak values. But the validity of building up a substantial wake-field amplitude by stimulated wake-field emission from a number of driving bunches of modest charge will be demonstrated here. It is this that is proposed as a new means for achieving high wake-field acceleration gradients, without need for bunches of exceptionally high charge.

Ruth *et al.* [7] have modeled the wake field from multiple driving bunches, assuming that successive bunches radiate wake-field energy identically. In their model, the composite wake field of a train of bunches would be a linear superposition of individual wake-field amplitudes. Synchronism of multiple driving bunches with the wake-field period has been discussed previously by Onishchenko *et al.* [8], who have experimentally observed intense radiation attributable to the progressive buildup of a strong wake field. Finally, Bane, Chen, and Wilson [9] have considered collinear wake-field acceleration generally, and show that a ''transformer ratio'' (i.e., the ratio of wake field to drag field for a bare bunch) greater than two is possible in multimode structures where the mode eigenfrequencies ω_n are equally spaced, with $\omega_n = \omega_0(2n+1)$; this signifies that particles can be accelerated to energies greater than twice the energy of particles in the driving bunch. In S-WAC, the multimode aspect of the dielectric waveguide chosen is a crucial factor since, as will be demonstrated below, the waveguide eigenfrequency spectrum can be designed to nearly fit the relationship $\omega_n = \omega_0(2n+1)$.

In this paper, we shall present the wake-field theory for a simplified slab geometry driven by a bunched sheet beam. Numerical examples are provided to show how a well-defined, spatiotemporally localized wake field may be produced using high dielectric constant low-loss material, providing the geometrical variables are correctly chosen. We discuss how wake-field amplitudes may be further enhanced by the superposition of contributions from successive drive bunches, together with stimulated emission. We provide a numerical example showing acceleration of test electrons from 30 to 155 MeV, in a 200 cm long two-dimensional dielectric waveguide, using 2-nC/mm drive bunches. For this example, the transformer ratio is 4.7. Further examples are given in which drive bunches are removed from the interaction once they have lost most of their energy, but before they can slip into accelerating phases and drain wake-field energy, and thereby reduce the available accelerating gradient for the test bunch.

II. WAVEGUIDE MODES AND WAKE-FIELD STRUCTURE

The model analyzed here is simplified to bring out the essential physics. Thus a two-dimensional waveguide is considered, in which two parallel slabs of dielectric are separated by a small vacuum gap, and in which the outer surfaces of the slabs are sheathed in a lossless conductor. The relative dielectric constant κ for the slabs is assumed to be independent of frequency. The geometry is depicted in Fig. 1, and all quantities are taken to be independent of y. The electrons are injected along the z axis in sheet bunches, with charge density given by $\rho(x,z,t) = -eN\delta(x)h(z-\nu t)$, where e is the magnitude of the electron charge, N is the charge number per unit length in the y direction along the sheet, $\delta(x)$ is the transverse charge distribution, assumed to be of infinitesimal width in x, and $h(z-\nu t)$ is the longitudinal charge distribution for bunch particles moving at axial speed ν. Simplification is afforded when the geometry is two dimensional (2D), with orientation of the dielectric as shown in Fig. 1. In this case, orthonormal wave functions can be found for the electromagnetic fields that separate into TE^x and TM^x classes with respect to the x axis; these are also known as LSE and LSM modes [10]. In 2D geometry, only the TM^x mode has an axial electric field; this is the mode considered here. For 3D geometry, when the waveguide shown in Fig. 1 is closed from above and below by conducting planes normal to the y axis, both TE^x and TM^x modes must be included. In cylindrical geometry, only axisymmetric excitations separate into TE and TM modes, and generally one must deal with hybrid modes [1]. For the geometry shown in Fig. 1, conditions can be found where all TM^x modes have phase velocities equal to ν, corresponding to wake fields that move in synchronism with the electron bunches. The field components for the complete orthonormal TM^x mode set are given by

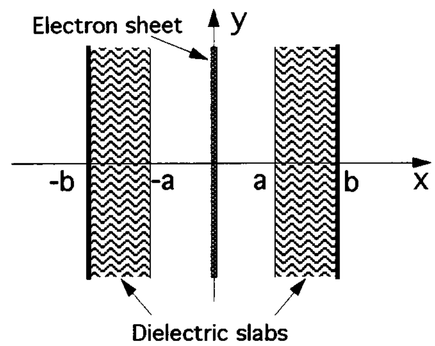

FIG. 1. Geometry for the two-dimensional dielectric-lined waveguide.

$$E_z(x,z,t) = \sum_{m=0}^{\infty} E_m \frac{f_m(x)}{\alpha_m} e^{-i\omega_m z_0/\nu}, \tag{1}$$

where

$$f_m(x) = \frac{1}{\sin p_m(b-a)} \times \begin{cases} \cosh k_m a \ \sin p_m(b+x), & -b \leqslant x \leqslant -a \\ \cosh k_m x \ \sin p_m(b-a), & -a \leqslant x \leqslant a \\ \cosh k_m a \ \sin p_m(b-x), & a \leqslant x \leqslant b, \end{cases} \tag{2}$$

and $z_0 = z - \nu t$;

$$E_x(x,z,t) = i\sum_{m=0}^{\infty} E_m \frac{g_m(x)}{\alpha_m} e^{-i\omega_m z_0/\nu}, \tag{3}$$

where

$$g_m(x) = \frac{\gamma}{\kappa \cos p_m(b-a)} \times \begin{cases} -\sinh k_m a \ \cos p_m(b+x), & -b \leqslant x \leqslant -a \\ \kappa \sinh k_m x \ \cos p_m(b-a), & -a \leqslant x \leqslant a \\ \sinh k_m a \ \cos p_m(b-x), & a \leqslant x \leqslant b, \end{cases} \tag{4}$$

and

$$H_y(x,z,t) = c\beta E_x(x,z,t) \begin{cases} \kappa, & -b \leqslant x \leqslant -a \\ 1, & -a \leqslant x \leqslant a \\ \kappa, & a \leqslant x \leqslant b. \end{cases} \tag{5}$$

The normalizing constant is

$$\alpha_m = 1 + \frac{\sinh(2k_m a)}{(2k_m a)} + \cosh^2(k_m a)\left[\frac{\kappa(b-a)}{a\ \sin^2 p_m(b-a)} - \frac{\tanh(k_m a)}{(k_m a)}\right];$$

$\beta = v/c$, $\gamma = (1-\beta^2)^{-1/2}$, the eigenfrequencies are $\omega_m = c\beta p_m/\sqrt{\kappa\beta^2-1}$, and $k_m = \omega_m/c\beta\gamma = p_m/\gamma\sqrt{\kappa\beta^2-1}$. The (evanescent) transverse wave number in the vacuum is k_m, and the (real) transverse wave number in the dielectric is p_m, and $\omega_m = c\beta k_{z,m}$. For the fields given by Eqs. (1)–(5), orthonormalization is obtained in the form

$$\int_{-b}^{b} dx E_{z,m} D^*_{z,n} = \delta_{mn} \frac{a}{\sqrt{\alpha_m \alpha_n}} \varepsilon_0 E_m E_n \times \exp[-iz_0(\omega_m - \omega_n)/v], \tag{6}$$

where $D^*_{z,n} = \varepsilon E^*_{z,n} = \kappa\varepsilon_0 E^*_{z,n}$ in the dielectric slabs and $D^*_{z,n} = \varepsilon_0 E^*_{z,n}$ in the vacuum gap. The dispersion relation is found to be

$$p_m \tanh(k_m a) = \kappa k_m \cot[p_m(b-a)]. \tag{7}$$

It is noted that one can have eigenfrequencies with nearly equal spacing, since $p_m(b-a) \to (n+1/2)\pi$ as $\kappa \to \infty$. As $m \to \infty$ the asymptotic eigenfrequency spacing approaches $\Delta\omega = \pi c\beta[(b-a)\sqrt{\kappa\beta^2-1}]^{-1}$. The wake field is more strongly peaked and more closely periodic in z_0 as the eigenfrequencies become more nearly periodic, i.e., as a higher value of κ is used.

To find wake fields induced by an electron bunch, one expands in orthonormal modes the solution of the inhomogeneous wave equation,

$$\left[\frac{\partial^2}{\partial x^2} + \frac{\partial^2}{\partial z^2} - \frac{\kappa(x)}{c^2}\frac{\partial^2}{\partial t^2}\right] E_z(x,z,t) = S_z(x,z,t), \tag{8}$$

with the source function

$$S_z(x,z,t) = \mu_0 \frac{\partial j_z}{\partial t} + \frac{1}{\varepsilon_0}\frac{\partial \rho}{\partial z},$$

where the z component of the current density is $j_z(x,z,t) = v\rho(x,z,t)$, and where $S_z(x,z,t) = 0$ for $|x| \geq a$. A complete solution can be constructed from fields as given in Eq. (1), since these are solutions of Eq. (8) with $S_z(x,z,t) = 0$ everywhere. We expand the solution of Eq. (8) in the interval $-b \leq x \leq b$ in a Fourier series:

$$E_z(x,z,t) = \sum_{m=0}^{\infty} \frac{1}{\alpha_m} f_m(x) \int_{-\infty}^{\infty} dk\ A_m(k) e^{-ikz_0}. \tag{9}$$

Inserting Eq. (9) into Eq. (8), and multiplying both sides by $w(x) D^*_{z,n}(x,z,t)$ gives

$$A_m(k) = \frac{1}{2\pi\alpha_m(k^2 - \omega_m^2/v^2)} \int_{-b}^{b} dx' \int_{-\infty}^{\infty} dz'_0 S_z(x',z'_0) \times \kappa(x') f_m(x') w(x') e^{ikz'_0}. \tag{10}$$

Then, integrating over k, with due regard for the choice of the contour of integration consistent with causality, and invoking Eq. (6) yields

$$E_z(x,z,t) = \sum_{m=0}^{\infty} \int_{-b}^{b} dx' \int_{-\infty}^{\infty} dz'_0 S_z(x',z'_0) G_m(x,z_0;x',z'_0), \tag{11}$$

where the Green's function $G_m(x,z_0;x',z'_0)$ is

$$G_m(x,z_0;x',z'_0) = \frac{-iv\kappa(x')}{2\omega_m \alpha_m a} w(x') f_m(x') f_m(x) \times e^{-i\omega_m|z_0 - z'_0|/v}, \tag{12}$$

and the weighting factor is $w(x) = [(\kappa\beta^2-1)^{-1}, -\gamma^2, (\kappa\beta^2-1)^{-1}]$ in the intervals $[(-b \leq x \leq -a), (-a \leq x \leq a), (a \leq x \leq b)]$, respectively.

For a rectangular bunch $\rho(x,z,t) = -Ne\delta(x)/\Delta z$ in the interval $z_0 - \Delta z/2 \leq z \leq z_0 + \Delta z/2$, and $\rho(x,z,t) = 0$ otherwise, one finds for the coherent spontaneous wake field from a bunch containing N electrons the result

$$E_z(x,z,t) = -E_0 \sum_{m=0}^{\infty} \frac{f_m(x)}{\alpha_m} \frac{\sin(\omega_m \Delta z/2v)}{(\omega_m \Delta z/2v)} e^{-i\omega_m z_0/v}. \tag{13}$$

While for a Gaussian bunch of N electrons with $\rho(x,z,t) = [Ne\delta(x)/\Delta z]\exp[-(z_0/\Delta z)^2]$, one finds the result

$$E_z(x,z,t) = -E_0 \sum_{m=0}^{\infty} \frac{f_m(x)}{\alpha_m} e^{-(\omega_m \Delta z/2v)^2} e^{-i\omega_m z_0/v}. \tag{14}$$

In Eqs. (13) and (14), $E_0 = -Ne/2\varepsilon_0 a$ is a measure of the Coulomb field of the bunch, and causality dictates that the results are valid only behind the bunch, i.e., for $z_0 \leq 0$; ahead of the bunch the fields are, of course, zero.

The fields for the Gaussian bunch case have been evaluated for a waveguide with $a = 0.30$ cm, $b = 1.147$ cm, $\kappa = 10.0$, $\Delta z = 3.0$ mm, $-Ne = Q = -2$ nC/mm, and $\gamma = 60$. A relative dielectric constant of $\kappa = 10.0$ is close to the value of 9.6 for alumina, the material that could be used to construct a proof-of-principal device. It is assumed in this analysis that κ is independent of frequency. For these parameters, $E_0 = -37.7$ MV/m. The wake field is computed by including modes up to $m = 50$ in the sum in Eq. (14), although beyond the 12th mode the relative amplitudes are less than 1% of that for $m = 1$. For this case, the first eigenfrequency interval $(\omega_2 - \omega_1)/2\pi$ is 5.70 GHz, while the asymptotic interval $\Delta\omega/2\pi$ is 5.88 GHz; eigenfrequency intervals differ by at most 3.1%. The computed coherent spontaneous wake-field pattern for $E_z(x=0,z_0)$ of a single bunch is shown in Fig. 2

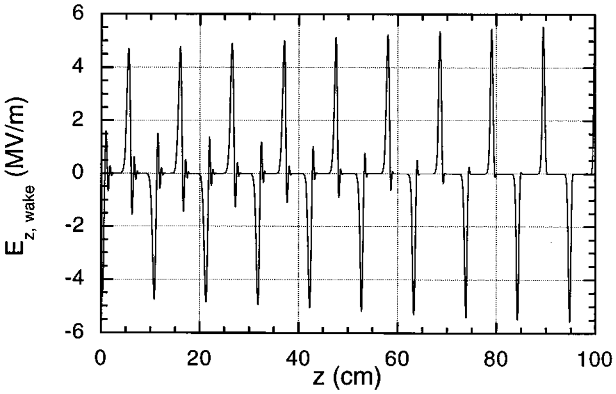

FIG. 2. Spontaneous wake field from a -2 nC/mm, 30 MeV, 3.0 mm long Gaussian sheet bunch after it has traveled 100 cm left-to-right in the 2D waveguide.

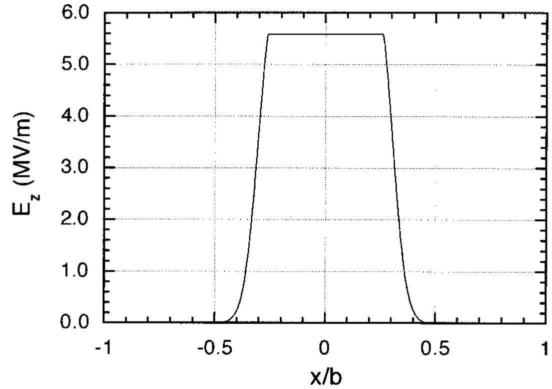

FIG. 4. Peak amplitude of the composite axial electric field for the wake-field example shown in Figs. 2 and 3.

for $0 \leqslant z \leqslant 100$ cm. The wake-field peaks are seen generally to alternate in sign; each is relatively concentrated in z and has a period of 10.5 cm, corresponding to the vacuum wavelength at 2.856 GHz, i.e., half the asymptotic frequency interval $\Delta\omega/2\pi$. The peak values of E_z for the first wake are -5.57 and $+5.54$ MV/m, and later wakes develop oscillatory precursors. Figure 3(a) shows the mode frequencies, and Fig. 3(b) shows the mode amplitudes A_m. It is clear that consideration of only the first few modes would give an incomplete picture of the wake-field structure. If the bunch length is decreased, the spectral width increases, and additional high-frequency structure develops; this is undesirable in connection with the superposition of several bunches. Also, the wider the bandwidth, the greater the influence of dielectric dispersion (neglected here). Below, we consider multiple injected bunches with parameters identical to this first bunch.

The transverse structure of the waveguide fields has also been computed for the example discussed in the preceding paragraph. Figure 4 shows the peak axial electric field $E_z(x,z_0=0)$. It is seen to be essentially independent of x in the vacuum gap, but it falls rapidly to zero in the dielectric regions. The peak transverse fields $E_x(x,z_0=z_m)$ and $H_y(x,z_0=z_m)$ have been computed from Eqs. (3) and (5), where $z_m=(2m+1)\pi\nu/2\omega_m$; these fields are depicted in Figs. 5 and 6. It is seen that the transverse fields are antisymmetric in x, essentially linear with x in the vacuum gap, but not insignificant in the dielectric regions. Figure 7 shows the Poynting vector $S_z=E_x\times H_y$, which is seen to vanish at $x=0$, to be discontinuous at the dielectric-vacuum interface, and to be largest near the conducting walls. Most of the power flow is seen to be within the dielectric, so that losses must be minimized to avoid undue heating. The wake-field power per unit height can also be found, as $P_{\rm wake}=\int_{-b}^{b}dxS_z(x)$; for the example discussed, one finds $P_{\rm wake}=80.0$ kW/mm. The wake-field power at any point in the waveguide is maintained at this level for the full 3.3 nsec

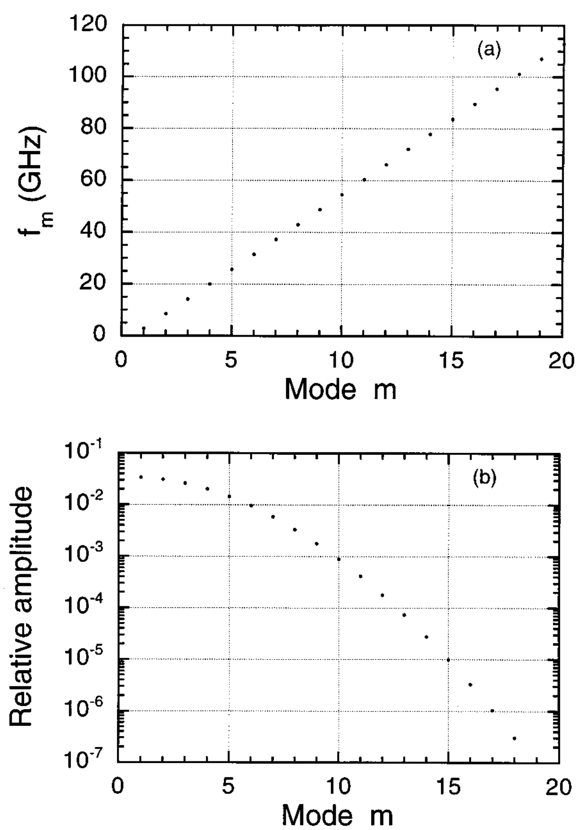

FIG. 3. (a) Wake-field mode frequencies; and (b) wake-field mode amplitudes.

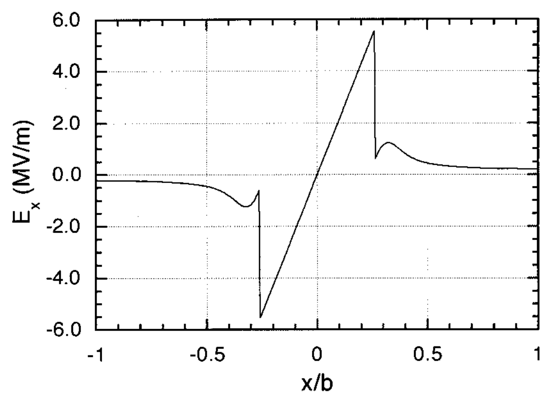

FIG. 5. Peak amplitude of the composite transverse electric field for the wake-field example shown in Figs. 2–4.

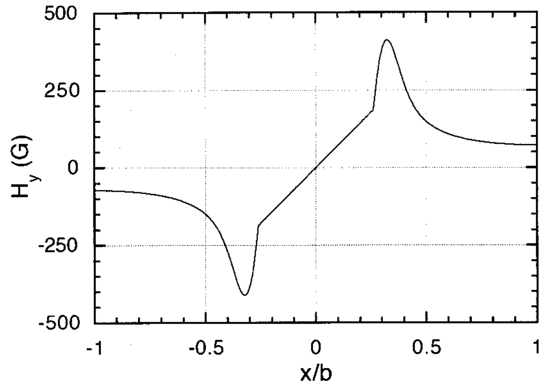

FIG. 6. Peak amplitude of the composite transverse magnetic field for the wake-field example shown in Figs. 2–5.

transit time of the bunch. In contrast, the peak power in the 10.0 psec bunch, defined as $P_b=(mc^2/e)(\gamma-1)(Q\nu/\Delta z)$, is 6.0 GW/mm.

III. STIMULATED EMISSION OF WAKE FIELDS BY A TRAIN OF BUNCHES

The choice of the particular dielectric-lined waveguide parameters in Sec. II is seen to result in a spacing of 10.5 cm between the first few sharply peaked positive polarity wake-field features. This spacing is equal to the interbunch spacing from a typical 2.856 GHz rf injector gun, or for that matter, a rf linac driven at this frequency. Therefore, if successive bunches were injected into the dielectric waveguide, the second bunch will find itself riding just on the crest of the first decelerating wake feature generated by the first bunch. Instead of generating only a coherent spontaneous Cherenkov wake as did the first bunch, the second bunch will be decelerated in the field of the first wake, and its energy will be radiated as additional stimulated Cherenkov energy, which builds up its own wake. Successive bunches will interact similarly. To make this quantitative, one calculates the incremental energy ΔW radiated into the waveguide by a bunch in advancing a distance Δz, and equates $\Delta W/\Delta z$ to the energy loss rate of the bunch. This loss rate is identified with a drag field E_{drag} acting on the bunch. Thus,

$$QE_{\mathrm{drag}}=\Delta W/\Delta z. \tag{15}$$

For a bare bunch, $E_{\mathrm{drag}}=E_{\mathrm{spon}}$, the drag field corresponding only to coherent spontaneous emission. But for a dressed bunch that follows behind N prior bunches, the drag field consists of the spontaneous drag field added to the combined wake fields of the preceding bunches. The total wake field is incremented by equating the sum of energies lost by all bunches to the change in wake-field energy, the latter being proportional to the square of the sum of wake-field amplitudes. It is also noted that perfect synchronism is assumed in the above simplified discussion, so that wake amplitudes (and not energies) are added constructively.

The rate of energy accumulation in wake fields behind any bunch (per unit height along the sheet bunch) is given by

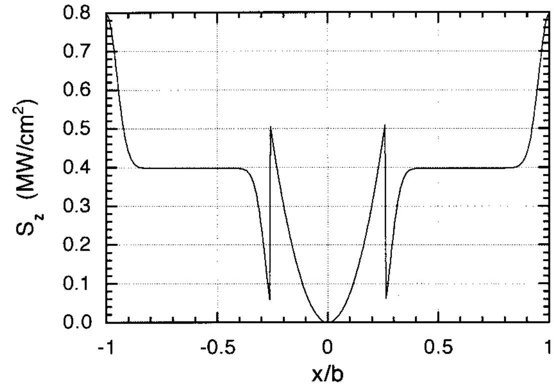

FIG. 7. Poynting vector for the wake-field example shown in Figs. 2–6.

$$\begin{aligned}\frac{dW}{dz}&=\frac{1}{4}\sum_{m=0}^{\infty}\int_{-b}^{b}dx\{\varepsilon(x)[E_{x,m}^2+E_{z,m}^2]+\mu_0H_{y,m}^2\}\\&=\frac{\varepsilon_0E_0^2b}{2}F\sum_{m=0}^{\infty}\frac{h^2(\xi_m)}{\alpha_m^2}\left\{\frac{a}{b}\gamma^2\left[\frac{\sinh(2k_ma)}{2k_ma}-\beta^2\right]\right.\\&\quad+\frac{b-a}{b}\frac{\kappa}{\kappa\beta^2-1}\left[\frac{\cosh(k_ma)}{\sin[p_m(b-a)]}\right]^2\\&\quad\left.\times\left[\frac{\sin[2p_m(b-a)]}{2p_m(b-a)}+\kappa\beta^2\right]\right\}.\end{aligned} \tag{16}$$

For a rectangular bunch, the structure factor is given by $h(\xi_m)=(\sin\xi_m/\xi_m)^2$; and for the Gaussian bunch, $h(\xi_m)$ $h(\xi_m)=\exp(-\xi_m^2)$, with $\xi_m=\omega_m\Delta z/2\nu$. In Eq. (16), F is a scale factor fixed by balancing the energy loss rate between drag on the bunch, and increase in the wake-field energy, as described in the prior paragraph. For a bare bunch $F=1$. This scaling procedure assumes that the source current and charge distributions in Eq. (8) remain constant during the interaction. If not, the individual mode amplitudes must be adjusted interatively; this amounts to introduction of a z-dependent structure factor $h(\xi_m)$ in equations such as Eqs. (13) and (14).

For the parameters chosen, Eq. (16) with $F=1$ gives $dW/dz=23.6\times10^{-4}$ J/m mm. (Note: the mm^{-1} comes from a 1 mm height up the sheet beam.) Equating dW/dz to the energy loss rate QE_{drag} gives $E_{\mathrm{drag}}=E_{\mathrm{spon}}=1.18$ MV/m for a bare bunch. The wake field induced by a bare bunch can be as high as 5.54 MV/m, as seen in Fig. 2, namely, 4.7 times the drag field. This factor, commonly referred to as the ''transformer ratio,'' is larger than the customary factor of 2 because of the multimode nature of wake fields that can participate in this case [9].

Now, when a second bunch is introduced into the waveguide at the peak of the first bunch wake field, it can be decelerated by up to $1.18+5.54=6.72$ MV/m, the sum of its own bare drag field associated with spontaneous emission, plus the wake field of the first bunch; this produces additional stimulated emission. Second bunch deceleration at a rate of 6.72 MV/m, i.e., 5.7 times that of a bare bunch, can clearly not proceed as far as the point $z=30/6.7=4.5$ m before which synchronism fails, due to slippage between the

TABLE I. Constructive superposition of wake fields for ten successive bunches in a 100 cm long dielectric waveguide, as described in the text. Initial $\gamma=60$. The simulation result shown in the last column is at the time the first bunch has reached $z=100$ cm.

Bunch number	$E_{\mathrm{drag},i}$ (MV/m)	$E_{w,i}$ (MV/m)	$\Sigma_i E_{w,i}$ (MV/m)	$\Sigma E_{w,i}$ (simulation) (MV/m)
1	1.18	5.54	5.54	5.82
2	6.72	8.79	14.33	13.69
3	15.51	10.34	24.67	23.05
4	25.85	11.12	35.79	32.80
5	36.97	11.56	47.35	42.66
6	48.53	11.84	59.19	52.49
7	60.37	12.04	71.23	62.20
8	72.41	12.17	83.40	71.80
9	84.58	12.28	95.68	81.25
10	96.36	12.36	108.04	90.61

particles and the wake fields as the bunch energy is depleted. The wake field of the second bunch adds its energy to that of the first bunch to give a combined wake field of 14.33 MV/m total. This addition of amplitudes only continues as long as synchronism is maintained between bunches and peak wake fields. Highly relativistic bunches can maintain synchronism while losing a larger fraction of their initial energy, as compared with bunches of lesser energy, since for the former velocity slip is lower, i.e., $\Delta\beta\approx\Delta\gamma/\gamma^3$.

In the following simple model for the buildup of a cumulative wake field from a driving bunch train, the bunches are taken as point charges that remain perfectly synchronized with the wake fields. The energy radiated into the wake field of the nth bunch can be written in terms of the net drag on the charge Q as

$$\frac{dW_n}{dz}=R\left[\left(\sum_{i=1}^{n} E_i\right)^2-\left(\sum_{i=1}^{n-1} E_i\right)^2\right]$$
$$=Q\left[E_{\mathrm{spon}}+\sum_{i=1}^{n-1} E_i\right]=QE_{\mathrm{drag}}, \qquad (17)$$

from which the combined wake field is found to be

$$\sum_{i=1}^{n} E_i=\left[\left(\sum_{i=1}^{n-1} E_i\right)^2+\frac{Q}{R}\left(E_{\mathrm{spon}}+\sum_{i=1}^{n-1} E_i\right)\right]^{1/2}. \qquad (18)$$

The factor R is obtained from the coefficient of the electric field squared in Eq. (16); $R=76.9$ nC/MV for the example cited. The individual wake field from the ith bunch is E_i.

Table I (except for the last column) shows a compilation from this (admittedly crude) estimate of the drag fields, individual wake fields and combined wake fields, as they would build up for ten injected bunches. The fifth column in the table lists, for purposes of comparison with the fourth column, the wake field obtained from the numerical study described in the next section. For comparison, the drag field that results when the transformer ratio is two is, for each bunch, an odd integer multiple of 1.18 MV/m, i.e., 1.18, 3.54, 5.90, 8.26 MV/m, etc. [7]. One can appreciate from Table I that participation of many copropagating modes, and stimulated emission from a periodic sequence of driving bunches, can increase dramatically the extraction of energy from the bunches, which in turn promotes the buildup of an intense overall wake field after passage of a relatively few moderate-charge driving bunches. These results suggest that stability problems can be avoided that may attend the propagation of a single drive bunch of very high charge that is needed to produce a strong wake field on its own.

IV. NUMERICAL SIMULATIONS

The conceptual model discussed in the prior section assumes perfect synchronism between driving bunches and peak wake fields, and assumes the wake-field amplitude to be uniform over the finite spatial extent of each bunch. The problem has been examined with greater accuracy in a numerical simulation, using 100 particles per bunch, and taking slip and actual wake-field amplitude variations into account. Particles in each 3.0 mm long bunch are injected each 350 psec (10.5 cm) around the peak of the wake field from prior bunches. The energy loss rate from each bunch is given by Eq. (16), with successive values of F found from the drag field on that bunch, i.e., from the sum of its spontaneous drag field E_{spon} and the net wake field from prior bunches. Particles in a given bunch obey the one-dimensional equation of motion $d\gamma/dz=(e/mc^2)E_{\mathrm{drag}}$, evaluated at each particle's instantaneous location, where E_{drag} is obtained from Eq. (17). The initial energy of each bunch is chosen with $\gamma_{\mathrm{initial}}=60$, or about 30 MeV. In this model, the bunches—now distributed spatially—will lose energy and thus can slip with respect to the wake fields. Motion in the x-y transverse plane is neglected.

In Figs. 8 and 9 are shown the results of injecting a test electron bunch of small charge into the accelerating phase of the wake field set up by the passage of ten prior driving bunches in a structure 100 cm in length, taking the initial energy of all test electrons to be about 30 MeV (i.e., $\gamma_{\mathrm{initial}}=60.0$). Beam loading by the test bunch is neglected, so it is assumed that the test bunch charge is very small. The parameters of this simulation are identical to those pertaining to Fig. 2. Figure 8(a) shows the buildup of the wake field from the ten driving bunches, and Fig. 8(b) shows the location of the finite-length test electron bunch to be accelerated. The test bunch (No. 11) enters behind the tenth drive bunch at the peak accelerating field, after the first drive bunch has traveled $\nu_0 t=100$ cm. Bunch velocities are initially close to c (i.e., $0.99972c$ for $\gamma_{\mathrm{initial}}=60.0$). The location of the drive bunches at this instant is indicated on Fig. 8(a). As the drive bunches proceed through the 100 cm long device, the energy of the test electrons increases. In Fig. 9 we plot the energy of every other drive bunch and the energy of the accelerated test bunch (No. 11). After $\nu_0 t=200$ cm, the 94.5 cm train of drive bunches has moved out of the structure, and the accelerated electrons are just departing. Their energy has been increased to 100 MeV, with an average acceleration gradient of about 70 MV/m. The value 70 MV/m is greater than ten times the 5.6 MV/m peak wake field of a single bunch. This shows that a stronger wake field can be produced by a multibunch train, than by a single bunch containing the total charge of all the bunches. The peak wake field in the struc-

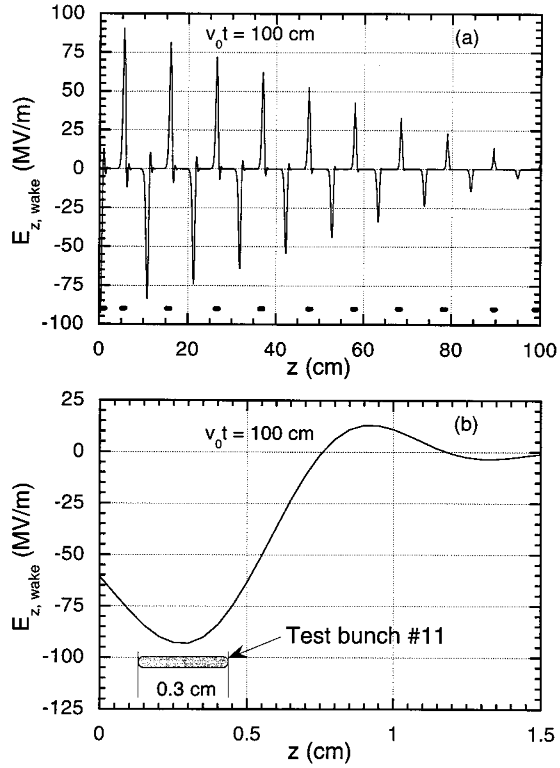

FIG. 8. (a) Cumulative wake-field set up by ten identical successive bunches, at the time the first bunch has moved 100 cm along the waveguide. The positions of the bunches are indicated by the black dots in the figure. (b) Location of the test bunch (No. 11) in the accelerating wake field near the entrance of the waveguide, when the first bunch has moved 100 cm.

ture, 90.6 MV/m, does not exceed known theoretical [6] or experimental breakdown limits [11]. Table I shows, for comparison, that the simplified model predicts a total wake field of 108 MV/m after the 10th driving bunch. The later drive bunches show energy depletion, and indeed by $\nu_0 t = 120$ cm they decrease in energy so that there is first a slippage off the wake-field maximum, followed by a further slippage into the following accelerating phase, after which the drive bunch energy begins to increase again. In this way, the maximum wake-field amplitude is eroded downstream. In Fig. 10 is shown the energy spread of the accelerated electrons, about 14% over the bunch length of 3 mm, due to the variation of the accelerating wake field over the finite-extent of the test bunch; forward slippage of the test bunch is insignificant.

The wake-field power at any point in the waveguide builds up in a stepwise fashion, over a 3.3 nsec interval, to a level of 19.4 MW/mm. [This value is found by multiplying the single-bunch value of 80.0 kW/mm by the square of the ratio of peak wake-field amplitudes for ten bunches and one bunch, namely, $(90.61/5.82)^2 = 242.4$.] The 19.4 MW/mm level is maintained for a further interval of 3.3 nsec, after which it diminishes in stepwise fashion back to zero.

One can find an approximate upper limit for the ultimate energy to which a test bunch can be accelerated when it follows a train of driving bunches. This can be determined by calculating the wake-field energy available for absorption by the test bunch. For the example discussed in the preceding

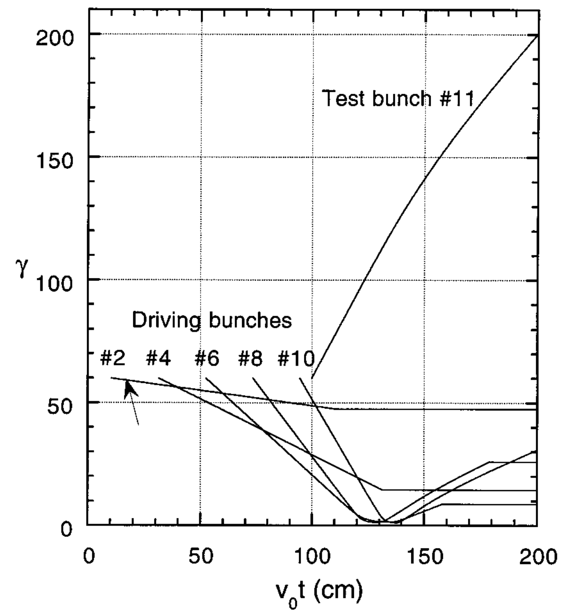

FIG. 9. History of the energy of various drive bunches and the test bunch, up to the time the test bunch just leaves the waveguide.

paragraphs, the wake-field energy is 174 mJ behind the test bunch at $\nu_0 t = 200$ cm, i.e., when the first drive bunch is leaving the waveguide and when the test bunch energy is 101.7 MeV. If, for example, the test bunch charge were 0.5 nC, it would have absorbed 36 mJ in acquiring 72 MeV up to $\nu_0 t = 200$ cm, so about 138 mJ is still available. Thus the test bunch could in principal acquire another 272 MeV, for a maximum ultimate energy of 374 MeV. However, as the test bunch approaches this energy, beam loading will have depleted the wake-field energy, and the acceleration gradient will have fallen below the 56 MV/m value it experienced at $\nu_0 t = 200$ cm. Thus the distance necessary to reach, say, 350 MeV will be greater than 6 m.

From the results shown in Figs. 9 and 10, it is apparent that one should endeavor to eliminate driving bunches from the system after their energy has decreased so much that they begin to slip into an accelerating field. The consequence of eliminating spent driving bunches has been examined by numerically decoupling a driving bunch from the computation before reacceleration can take place. In Fig. 11, we show a

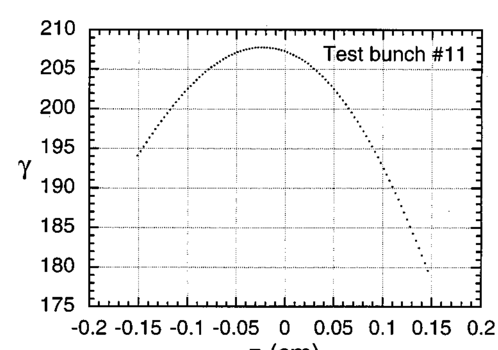

FIG. 10. Energy spread of electrons in the test bunch at $\nu_0 t = 200$ cm.

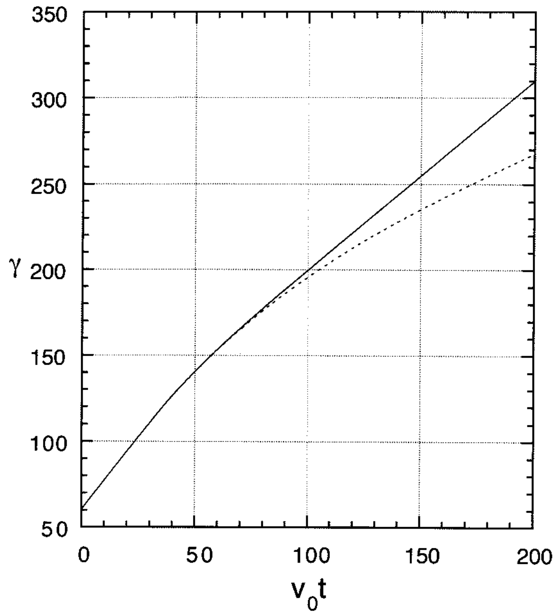

FIG. 11. Energy of the test electrons vs $\nu_0 t$ for two cases. The dotted line is for the case described in Figs. 8 and 9, but carried out for a 200 cm long waveguide, where the bunches are left in the system the entire length. The solid line is for the case where the drive bunches are eliminated after moving 100 cm along the 200 cm long waveguide.

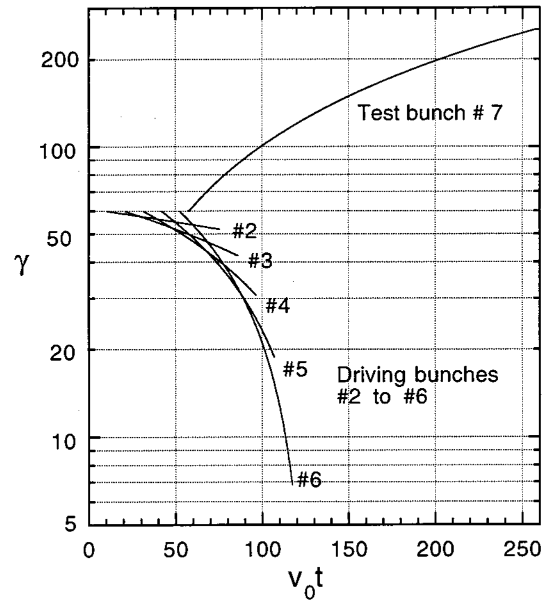

FIG. 12. History of the energy of drive bunches in a six bunch train, when the bunches are eliminated at $z=65$ cm. The total waveguide length is 200 cm, and the average accelerating wake field produced is 42.5 MV/m.

result obtained using a 200 cm long dielectric structure, where the ten drive bunches are abruptly deflected out after traveling 100 cm. We find that the energy of the test particles increases steadily to 155 MeV after traversing the system. This compares favorably with what happens when one leaves the drive bunches in for the full 200 cm, where the test particles only reach an energy of 135 MeV. When drive bunches decrease in energy so that particle speeds are significantly reduced below c, their wake fields will not remain synchronized with the fields of the more energetic drive bunches; the net wake field could lose its spatiotemporal coherence. But, since stimulated wake-field emission is proportional to the local net field of prior bunches, this will fall rapidly once a driving bunch loses synchronism. Nevertheless, the reacceleration of drive bunches will drain wake-field energy and diminish the accelerating field available for the test bunch, as seen in Figs. 9 and 11. One cure for this is to deflect away a drive bunch when its energy falls below a certain limit, e.g., using a transverse magnetic field that is too small to deflect the orbit of the test electrons appreciably, and then using a second magnet to correct the orbit of the test bunch. We have run another case to show this, as depicted in Fig. 12, where six bunches are deflected out at $z=65$ cm. The energy of the (initially) 30 MeV drive bunches does not fall below 3 MeV, and the test electrons reach 126 MeV at the end of the 200 cm long structure, for a mean accelerating gradient of 48 MV/m. As in the prior example, this value is seen to be more than six times the wake-field amplitude 5.6 MV/m of a single bunch, showing again that a stronger wake field can be generated by a multibunch train, than by a single bunch whose charge is equal to the total charge of all bunches in the train.

Deflection of drive bunches when their energy falls, without seriously affecting test bunches, will doubtless require careful design and control of the deflecting field, and will require slots in the dielectric waveguide for egress of spent drive bunches. An alternative is to allow drive bunches to move rectilinearly, but to deflect the wake fields into a second waveguide where the test bunch also moves rectilinearly, a scheme that resembles one suggested in Ref. [12]. Either of these approaches lends itself to multistage acceleration, in which achievement of energies of interest for high-energy particle physics experiments is possible. In any case, it is clear that collinear transport of drive bunches and test bunches will impose limitations on the net acceleration one can achieve with a wake-field accelerator, as others have already concluded [9].

V. DISCUSSION

The model presented in this paper is admittedly a simplified one, in that it is a two-dimensional waveguide and a bunched sheet beam that were discussed and analyzed. Clearly a practical arrangement will be three-dimensional, utilizing either a dielectric-lined cylindrical waveguide or a rectangular waveguide containing one or two dielectric slabs. The analysis should be extended to these cases to examine their potential for producing wake fields similar to those described in this paper. Preliminary study [13] of dispersion in a cylindrical dielectric-lined waveguide has shown that eigenmodes with phase velocities close to c will have minimum deviations in eigenfrequency spacing that are somewhat more than double the deviations for planar waveguide [cf. Fig. 3(a)]. But cylindrical waveguides may not allow transformer ratios as high as those found in this paper, since radiated wake field energy must fill a larger volume proportionally than for the two-dimensional case. The possibility of employing advanced materials with dielectric constant κ

greater than 10 should also be examined since, for short driving bunch lengths, higher κ results in sharper wake-field peaks. It also may be that a multilayer dielectric liner could be used to introduce compensation for the dispersion of a single-layered liner, but preliminary study of this question has so far yielded inconclusive results.

Significant wake-field power flow has been found for the train of ten driving bunches, namely, 19.4 MW/mm. The corresponding value for a cylindrical waveguide could exceed 100 MW, in about a dozen TM_{0m} modes ranging in frequency from 2.856 to perhaps 50 GHz, and in a pulse about 10 nsec long. Comparable power and pulse width with such a spectrum cannot be obtained from a conventional rf source, without a complex system for pulse compression and harmonic multiplication. But a limitation exists in peak and average power capability for a dielectric waveguide, on account of dielectric breakdown and bulk heating from volumetric losses.

Transverse wake fields have not been addressed in the analysis presented here. But recently, it was shown that these vanish in ideal planar geometry as $\gamma \rightarrow \infty$ [14]. For dielectric-lined cylindrical waveguides, transverse fields from a single driving bunch have been examined [3,4]; it was found that these can be weaker than in traditional disk-loaded waveguides. Nevertheless, transverse wake fields will need to be analyzed for S-WAC to determine how they build up in a multibunch train, and how they influence beam stability.

Another assumption underlying the calculation is that wake fields continue to travel with the speed of the 30 MeV particles, even when a drive bunch is significantly decelerated. In view of the highly relativistic motion and the finite length (100 cm) along the first part of the system, this is a good assumption until the drive bunch energy has been reduced below a few MeV, as discussed above. Additionally, it would be necessary to include a variable structure factor $h(\xi_m)$ [see Eq. (16)] to account for distortions in bunch distribution when severe energy depletion sets in. On the other hand, accelerated particles always travel very close to c and, by the time 200 cm has been reached, the accelerated electrons have not slipped significantly ahead of an accelerating wake-field pulse. Extension of the theory to include beam loading by a test bunch is necessary to obtain accurate acceleration lengths. It will also be necessary to examine means to deflect away either the spent driving bunches, or to diffract away the wake field, once the driving bunches begin to slip. These improvements to the theory are needed to allow optimization of strong multibunch wake fields, with acceleration of one or more test bunches. But, the above limitations notwithstanding, it seems reasonable to expect that the simplified calculations presented in this paper can provide an adequate guide for further detailed calculations, and ultimately for the design of a convincing proof-of-principal ''two-beam'' stimulated dielectric wake-field accelerator experiment.

ACKNOWLEDGMENTS

Useful discussions that led to important suggestions were held with A. K. Ganguly and Changbiao Wang. This research was supported by the U.S. Department Of Energy, Division of High Energy Physics.

[1] C. T. M. Chang and J. W. Dawson, J. Appl. Phys. **41**, 4493 (1970).
[2] B. M. Bolotovskii, Usp. Fiz. Nauk **75**, 295 (1961) [Sov. Phys. Usp. **4**, 781 (1962)].
[3] K.-Y. Ng, Phys. Rev. D **42**, 1819 (1990).
[4] M. Rosing and W. Gai, Phys. Rev. D **42**, 1829 (1990).
[5] W. Gai, P. Schoessow, B. Cole, R. Konecny, J. Norem, J. Rosenzweig, and J. Simpson, Phys. Rev. Lett. **61**, 2756 (1988).
[6] P. Sprangle, B. Hafizi, and R. F. Hubbard, Phys. Rev. E **55**, 5964 (1997).
[7] R. D. Ruth, A. W. Chao, P. L. Morton, and P. B. Wilson, Part. Accel. **17**, 171 (1985).
[8] I. N. Onishchenko, V. A. Kiseljob, A. K. Berezin, G. V. Sotnikov, V. V. Uskov, A. F. Linnak, and Ya. B. Fainberg, in *Proceedings of the 1995 Particle Accelerator Conference* (IEEE, New York, 1995), pp. 782–783.
[9] K. L. F. Bane, Pisin Chen, and P. B. Wilson, IEEE Trans. Nucl. Sci. **NS-32**, 3524 (1985).
[10] R. E. Collin, *Field Theory of Guided Waves* (IEEE Press, New York, 1991), Chap. 6.
[11] T-B. Zhang, T. C. Marshall, M. A. LaPointe, J. L. Hirshfield, and Amiram Ron, Phys. Rev. E **54**, 1918 (1996).
[12] W. Gai, A. D. Kanareykin, A. L. Kustev, and J. Simpson, Phys. Rev. E **55**, 3481 (1997).
[13] C. Wang (private communication).
[14] A. Tremaine, J. B. Rosenzweig, and P. Schoessow, Bull. Am. Phys. Soc. **42**, 1343 (1997).